

Biomimetic Syntheses of Rubialatins A, B and Related Congeners

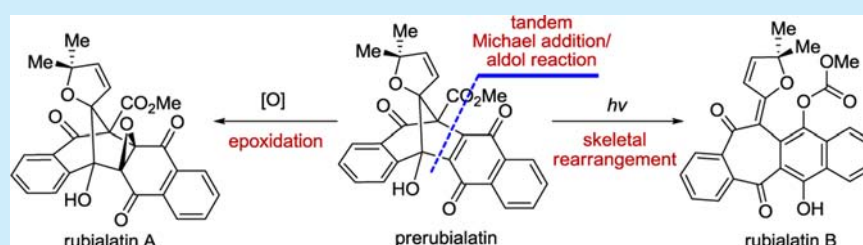
Hongzhi Yang,[†] Juan Feng,[†] Yuanhe Li,[†] and Yefeng Tang^{*,†,‡,§}

[†]The Comprehensive AIDS Research Center and Department of Pharmacology & Pharmaceutical Sciences, School of Medicine, Tsinghua University, Beijing, 100084, China

[‡]Collaborative Innovation Center for Biotherapy, Tsinghua University, Beijing 100084, China

[§]Collaborative Innovation Center for Biotherapy, State Key Laboratory of Biotherapy and Cancer Center, West China Hospital, West China Medical School, Sichuan University, Chengdu 610041, China

Supporting Information



ABSTRACT: The first total syntheses of rubialatins A and B, two newly discovered naphthohydroquinone dimers, were achieved with high efficiency and elegance through rationally designed biomimetic approaches. The tandem ring contraction/Michael addition/aldol reaction followed by oxidation enabled the rapid access of prerubialatin from readily available precursors, which then diverted into rubialatins A and B via epoxidation and photoinduced skeletal rearrangement, respectively. Moreover, several new rubialatin congeners were also obtained along the synthetic tour, some of which were proved to be authentic natural products.

Rubialatins A (1) and B (2) (Figure 1) are two naphthohydroquinone dimers recently isolated by Tian

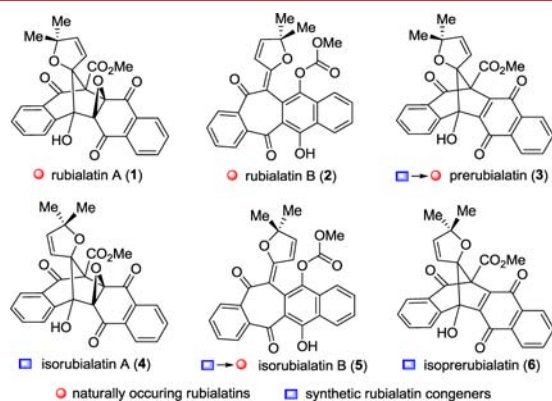


Figure 1. Rubialatins A, B and related congeners.

and co-workers from *Rubia alata Roxb.*,¹ a plant widely distributed in South China and used as a folk medicine. Different from the other naphthohydroquinone dimers identified in the same genus,^{2,3} both 1 and 2 bear unprecedented molecular architectures. As shown, 1 possesses a 6/6/5/6/6 polycyclic ring system which features a highly congested bicyclo[3.2.1]octane core attached with five consecutive stereogenic centers. Comparably, 2 has a planar 6/7/6/6 tetracyclic ring system coupled with a fully substituted

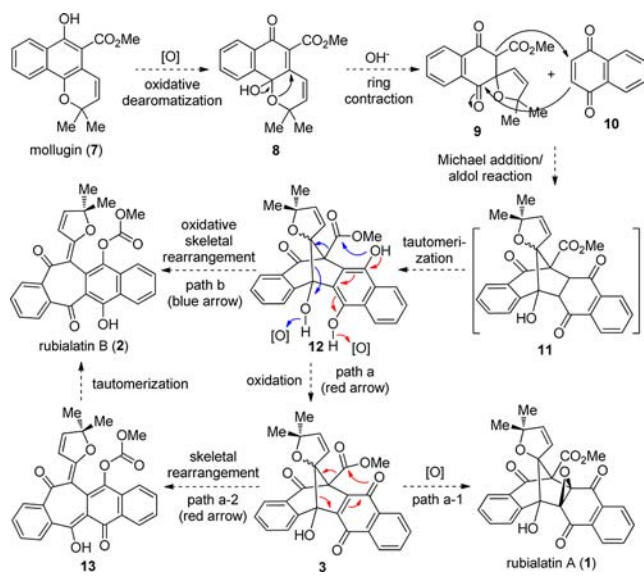
cycloheptane-1,4-dione core (Figure 1). Preliminary biological studies showed that 2 displayed moderate cytotoxicity against several tumor cell lines. Additionally, 1 could inhibit TNF- α induced NF- κ B activation, while 2 activates the NF- κ B pathway with the existence of TNF- α . Not surprisingly, the unique molecular architectures and promising biological profiles of 1 and 2 render them attractive targets for total synthesis. Herein, we report the first total syntheses of 1 and 2 based on rationally designed biomimetic approaches. Meanwhile, our synthetic effort led to the discovery of several new rubialatin congeners, including prerubialatin (3), isorubialatin A (4), isorubialatin B (5), and isoperubialatin (6) (Figure 1). Of note, two of them, 3 and 5, proved to be authentic natural products which were overlooked in the previous isolation program.

Our strategic planning for the syntheses of 1 and 2 was inspired by their plausible biosynthetic origins which were first suggested by Tian and co-workers and further rationalized by us. As depicted in Scheme 1, Mollugin (7),⁴ a coexisting substance found in the same plant as 1 and 2, could undergo oxidative dearomatization to afford 8 which readily converts to 9 via ring contraction under basic conditions. The union of 9 and 10 via a tandem Michael addition/aldol reaction would yield intermediate 11 which spontaneously undergoes tautomerization to give hydroquinone 12. At this point, 12 could first advance to quinone 3 via oxidation, which then

Received: January 31, 2015

Published: February 27, 2015

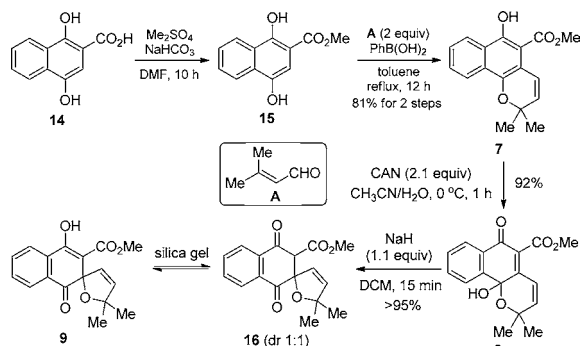
Scheme 1. Proposed Biosynthetic Origins of Rubialatins A and B



diverts into rubialatin A (1) via epoxidation (path a-1) or rubialatin B (2) via skeletal rearrangement (path a-2). Alternatively, 12 could also directly transform to 2 via an oxidative skeletal rearrangement (path b), as suggested in the isolation paper.¹

Our investigations started from the preparation of fragment 9 (Scheme 2). Thus, mollugin (7) was first synthesized from the

Scheme 2. Preparation of Fragment 9/16

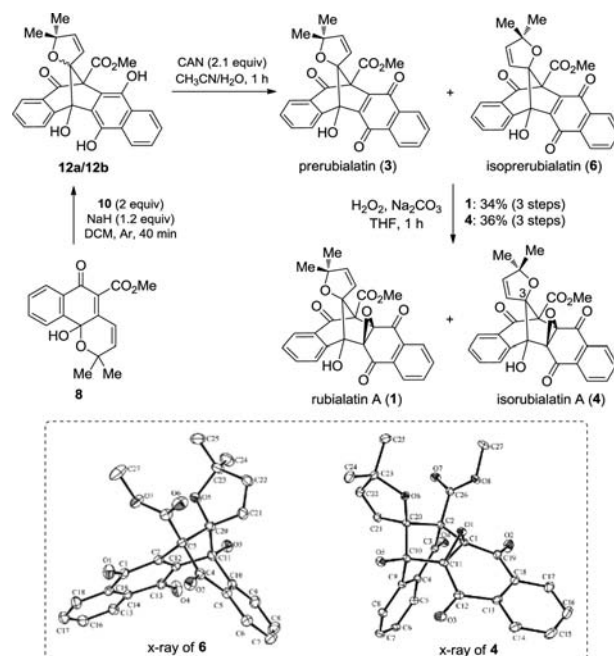


commercially available 1,4-dihydroxy-2-naphthoic acid (14) via two steps based on the known method.⁵ The oxidative dearomatization of 7 with cerium ammonium nitrate (CAN) in $\text{CH}_3\text{CN}/\text{H}_2\text{O}$ proceeded smoothly to afford 8 in 92% yield. Gratifyingly, it was found that 8 could spontaneously undergo ring contraction to yield a mixture of 16 and its tautomer 9 when purified by chromatography. Subsequently, we found that such a process could be accelerated under basic conditions. Thus, the treatment of 8 with NaH (1.1 equiv) in DCM for 15 min resulted in the formation of 16 (dr = 1:1) in nearly quantitative yield (>95%).

With the synthesis of 16 secured, we then attempted the proposed tandem Michael–aldol reaction. Notably, we recently completed the total synthesis of incarvilleatone, wherein a biomimetic tandem oxa-Michael/Michael/aldol reaction was achieved by using the combination of NaH/DCM.⁶ Given the resemblance between these two cases, we first examined that

condition in the current scenario. To our delight, upon treatment of 16 and 10 with NaH (1.2 equiv) in DCM under an argon atmosphere for 40 min, the expected reaction did take place, affording a mixture of C-3 epimers 12a/12b (1:1.6 ratio) in 20% combined yields together with 50% of unchanged starting material (Table S1, entry 1, Supporting Information). To our delight, we subsequently found that the direct use of 8 instead of 16 in the reaction gave a better result, with 12a/12b obtained in 78% combined yields (Table S1, entry 2). Of note, small amounts of the quinone derivatives 3 and 6 (ca. 10%) were also detected at this stage, which might respectively generate from 12a and 12b via autoxidation when exposed to the air.⁷ Thus, without isolation the crude products were directly treated with excess amounts of CAN in $\text{CH}_3\text{CN}/\text{H}_2\text{O}$, which gave a mixture of 3 and 6 in nearly quantitative yield. The chromatographic separation of 3 and 6 turned out to be laborious due to the similar polarity. Thus, they were directly submitted to the next step for epoxidation (H_2O_2 , 1 N Na_2CO_3 , THF, 1 h), which finally delivered rubialatin A (1) and its C-3 epimer 4 in 34% and 36% isolated yields, respectively (Scheme 3).⁸

Scheme 3. Total Synthesis of Rubialatin A and Its Congeners

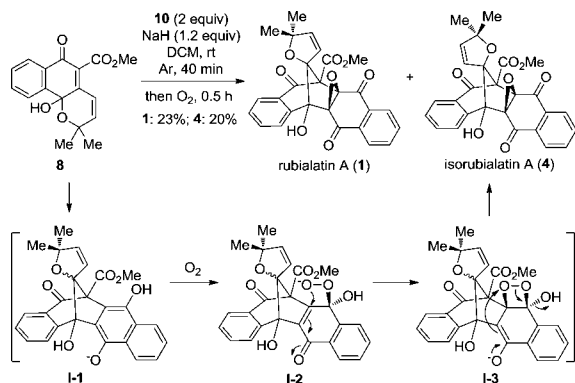


The spectroscopic data of synthetic 1 were in good agreement with those of the natural product. However, careful examination of the ^1H NMR spectrum of the natural sample revealed that it was contaminated with a minor component which was not mentioned in the isolation paper.¹ Interestingly, we found that its ^1H NMR signals are identical to those of synthetic compound 3, indicating that 3 is actually a natural product which was overlooked in the previous study (for details, see Supporting Information). In view of its apparent biosynthetic relationship to 1, 3 was named as prerubialatin. Similarly, 4 and 6, albeit having not been identified in nature so far, were respectively named as isorubialatin A and isopre-rubialatin. Their structures were confirmed by the crystallographic studies.⁹

Besides the stepwise synthesis of 1, a more operationally simple one-pot protocol was also developed by us. As shown in

Scheme 4, the treatment of **8** and **10** with NaH in DCM under an argon atmosphere for 40 min followed by exposure of the

Scheme 4. One-Pot Syntheses of Rubialatin A and Isorubialatin A



resulting reaction mixtures to O₂ for 0.5 h led to the formation of **1** and **4** in 23% and 20% yields, respectively. On the basis of some related precedents,¹⁰ we assumed that the naphthoxide **I-1**, once formed, could *in situ* convert to the peroxy anion **I-2** in the presence of O₂. **I-2** would then transform to the 1,2-dioxetane **I-3** via intramolecular 1,4-conjugate addition, which, after cleavage of the O–O bond of peroxide followed by release of H₂O, could afford **1** and **4**. Notably, the direct oxidation of hydroquinone to its quinone oxide with molecular oxygen was believed to be involved in the biosynthesis of Vitamin K oxide.^{10a–c} We assumed that such a process may also account for the biosynthetic origin of **1**.

Having achieved the synthesis of **1**, we then turned our attention to rubialatin B (**2**). Initially, the assumed oxidative skeletal rearrangement of **12a/12b** (path b, Scheme 1) was attempted. Although considerable effort was devoted to this subject, we failed to obtain promising results. Serendipitously, we found that the quinone **6** was unstable when kept in DCM for a long time and gradually transformed into some new products. To our delight, one of them (ca. 35%, entry 1, Table 1) turned out to be the desired product **2**, and the other proved to be **17** by the crystallographic study.⁹ This finding suggested that it was the quinones **3/6** instead of the hydroquinones **12a/12b** that might be the direct biosynthetic precursor of **2**. To find out the key factor that effected the rearrangement, we performed a systematic investigation. It was found that simply heating **6** in DCM at 100 °C (sealed tube) for 6 h failed to yield the desired product (entry 2), indicating that the reaction was unlikely promoted by thermal conditions. Next, both a Brønsted acid (e.g., HCl) and Lewis acid (e.g., ZnCl₂) were evaluated (entries 3 and 4).

However, all of them failed to promote the desired rearrangement. Instead, **6** gradually underwent epimerization on the C-3 stereocenter to afford a mixture of **3** and **6** (Scheme S-1, Supporting Information). Fortunately, we found that photoirradiation could notably accelerate the reaction. Indeed, upon irradiation with a metal–halide lamp (150 W) in DCM for 6–8 h, **6** was totally consumed, furnishing **2** in 51% yield together with 20% of **17** (entry 5). More pleasingly, when we directly irradiated **6** in its solid form,¹¹ a cleaner reaction was observed, with **2** obtained in a 56% yield (80% based on recovery of starting material) (entry 6). Furthermore, we found that besides **6** its C-3 isomer **3** could also undergo the skeletal

Table 1. Skeletal Rearrangement of **3/6** to Rubialatin B and Its Congeners

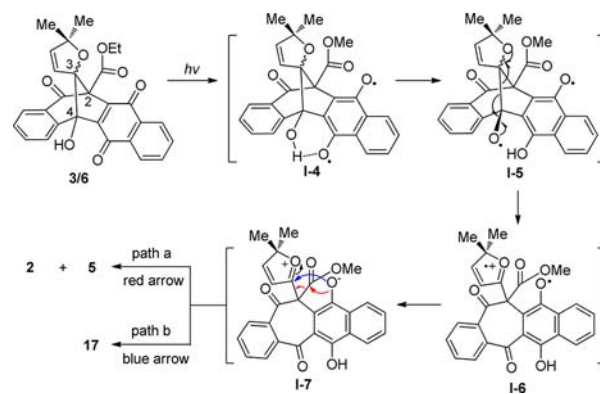
entry	conditions ^a	yield of products (%) ^b			
		2	5	17	6/3
1	6 , DCM, rt, 7 day	35	trace	15	28 (6)
2	6 , DCM, 100 °C, 6 h	trace			90 (6)
3	6 , 2 N HCl, DCM, 100 °C, 10 h	trace			90 (6/3 = 1/1)
4	6 , ZnCl ₂ (2 equiv), DCM, rt, 6 h	trace			95 (6/3 = 1/1)
5	6 , DCM, <i>hν</i> , rt, 8 h	51	trace	20	
6	6 , neat, <i>hν</i> , rt, 30 h	56	trace		30 (6)
7	3 , DCM, <i>hν</i> , rt, 8 h	60	trace		
8	3 , neat, <i>hν</i> , rt, 30 h	24	18%		50 (3)

^aAll reactions were performed with **6** or **3** (0.5 mmol) under the conditions as shown. ^bIsolated yields.

rearrangement when irradiated in DCM, providing the same product **2** in good yield (entry 7). Comparably, the photoreaction of **3** in the solid state appeared to be sluggish, only resulting in **2** in moderate yield even with a long reaction time (entry 8). A new product was observed in this reaction; however, attempts to obtain a pure sample for the structural assignment proved to be problematic, since it readily converted to **2** with further photoirradiation. Based on the following mechanistic rationalization as well as the experimental results, its structure was tentatively assigned as **5**.

Mechanistically, we assumed that the photoactivation of **3/6** could result in the formation of biradical intermediate **I-4** via *n*- π^* transition.¹² **I-4** then undergoes intramolecular 1,5-hydrogen atom transfer to give **I-5**, which subsequently evolves into **I-6** through homolytic cleavage of the C3–C4 bond. At this point, **I-6** could probably convert to the final products directly. However, it is more likely to transform to the zwitterion intermediate **I-7** first, which then diverts into **2** and **5** via 1,4-carboxylate migration (path a) or **17** via direct cyclization (path b) (Scheme 5).¹³

Scheme 5. Plausible Mechanism of Photoinduced Skeletal Rearrangement of **3** and **6**



While the above mechanistic rationalization appeared to be reasonable, another question deserved further consideration: why the rearrangement led to **2** as the sole or dominant product, although both **2** and **5** might generate from **I-7** via the rotation of the C2–C3 single bond. To answer the question, we conducted a computational study using B3LYP for geometry optimization and M06 for energy calculation with the 6-31++G(d, p) basis set. The result suggested that the isomer **2** is 11.2 kJ/mol more stable than the isomer **5** (for details, see Supporting Information). Thus, **I-7**, once formed, prefers to evolve into the thermodynamically more stable product **2**, especially for those reactions performed in solution. For the solid-state photoreaction of **3**, the isomer **5** may generate at first due to the restricted rotation of the C2–C3 single bond, which then isomerizes to **2** with further photoirradiation. Of note, both the experimental and calculation results are in good accordance with the fact that only rubialatin B (**2**) has been identified in nature. Nevertheless, when we carefully examined the ¹H NMR spectrum of the naturally occurring **2**,¹ we found that it was also contaminated with two tiny components, one of which had the same signals as those of **5** (for details, see Supporting Information). Thus, it is highly possible that **5** is indeed a naturally occurring substance, albeit probably in extremely low abundance.¹⁴ In this context, it was named as isorubialatin B. Similarly, **17** was tentatively named as rubialatin C.

In summary, the biomimetic syntheses of rubialatins A and B have been achieved, the key elements of which include a highly efficient tandem reaction involving ring-contraction/Michael addition/aldol reaction/autoxidation and a novel photoinduced skeletal rearrangement, respectively. Moreover, several new rubialatin congeners were also obtained along the synthetic tour, among which prerubialatin and isorubialatin B were found to be authentic natural products, and the others, as we anticipated, might be identified in nature some day. Taken together, the presented work not only sheds light on the biogenetic pathways of the rubialatin family of natural products but also paves the way to access ample material of the natural products as well as their analogs for further biomedical studies, which is ongoing in this laboratory.

■ ASSOCIATED CONTENT

Supporting Information

Detailed experimental procedures, characterization data, and copies of ¹H and ¹³C spectra of all products. This material is available free of charge via the Internet at <http://pubs.acs.org>.

■ AUTHOR INFORMATION

Corresponding Author

*E-mail: yefengtang@tsinghua.edu.cn.

Notes

The authors declare no competing financial interest.

■ ACKNOWLEDGMENTS

We acknowledge the financial support from the National Science Foundation of China (21102081, 21272133), Beijing Natural Science Foundation (2132037), and New Teachers' Fund for Doctor Stations, Ministry of Education (20110002120011). We also thank Prof. Ning-hua Tan (Kunming Institute of Botany, Chinese Academy of Sciences) for providing the original spectrum of the natural products.

■ REFERENCES

- (1) Zhao, S. M.; Wang, Z.; Zeng, G. Z.; Song, W. W.; Chen, X. Q.; Li, X. N.; Tan, N. H. *Org. Lett.* **2014**, *16*, 5576–5579.
- (2) (a) Qiao, Y. F.; Takeya, K.; Itokawa, H.; Iitaka, Y. *Chem. Pharm. Bull.* **1990**, *38*, 2896–2898. (b) Itokawa, H.; Ibraheim, Z. Z.; Qiao, Y. F.; Takeya, K. *Chem. Pharm. Bull.* **1993**, *41*, 1869–1872. (c) Ibraheim, Z. Z.; Gouda, Y. G. *Bull. Pharm. Sci., Assiut University* **2010**, *33*, 225–233.
- (3) For synthetic effort on naphthohydroquinone dimers, see: (a) Lumb, J. P.; Trauner, D. *J. Am. Chem. Soc.* **2005**, *127*, 2870–2871. (b) Lumb, J. P.; Choong, K. C.; Trauner, D. *J. Am. Chem. Soc.* **2008**, *130*, 9230–9231.
- (4) (a) Itokawa, H.; Mihara, H.; Takeya, K. *Chem. Pharm. Bull.* **1983**, *31*, 2353–2358. (b) Itokawa, H.; Qiao, Y.; Takeya, K. *Phytochemistry* **1991**, *30*, 637–640. (c) Ho, L. K.; Don, M. J.; Chen, H. C.; Yeh, S. F.; Chen, J. M. *J. Nat. Prod.* **1996**, *59*, 330–333.
- (5) Idhayadhulla, A.; Xia, L.; Leea, Y. R.; Kim, S. H.; Wee, Y.-J.; Lee, C.-S. *Bioorg. Chem.* **2014**, *52*, 77–82.
- (6) Zhao, K.; Cheng, G. J.; Yang, H. Z.; Shang, H.; Zhang, X. H.; Wu, Y. D.; Tang, Y. F. *Org. Lett.* **2012**, *14*, 4878–4881.
- (7) For autoxidation of hydroquinone to quinone in the presence of oxygen, see: (a) Kelly, T. R.; Field, J. A. *Tetrahedron Lett.* **1988**, *29*, 3545–3546. (b) Naruta, Y.; Nishigaichi, Y.; Maruyama, K. *J. Org. Chem.* **1988**, *53*, 1192–1199. (c) Hauser, F. M.; Hewawasam, P.; Rho, Y. S. *J. Org. Chem.* **1989**, *54*, 5110–5114. (d) Roginsky, V.; Barsukova, T. *J. Chem. Soc., Perkin Trans. 2* **2000**, 1575–1582.
- (8) Various other combinations of base and solvent were also evaluated; however, they failed to give satisfying results (Table S-1, Supporting Information). While the Michael–aldol reaction displayed no diastereoselectivity, we found that **1** and **4** could interconvert from each other under acidic conditions (Scheme S-1). Thus, both **1** and **4** could be obtained with higher overall yields through such interconversion.
- (9) CCDC 1042220 (**4**), 1042221 (**6**), and 1042227 (**17**) contain the supplementary crystallographic data for this paper. These data can be obtained free of charge from The Cambridge Crystallographic Data Centre via www.ccdc.cam.ac.uk/data_request/cif.
- (10) (a) Ham, S. W.; Dowd, P. *J. Am. Chem. Soc.* **1990**, *112*, 1660–1661. (b) Dowd, P.; Ham, S. W.; Geib, S. J. *J. Am. Chem. Soc.* **1991**, *113*, 7734–7743. (c) Dowdy, P.; Ham, S.-W.; Hershline, R. J. *Am. Chem. Soc.* **1992**, *114*, 7613–7617. (d) Ham, S. W.; Yoo, J. S. *Chem. Commun.* **1997**, 929–930. (e) Ham, S. W.; Lee, G. H. *Tetrahedron Lett.* **1998**, *39*, 4087–4090. (f) De, S. R.; Ghorai, S. K.; Mal, D. *J. Org. Chem.* **2009**, *74*, 1598–1604.
- (11) For selected examples of photoreaction in solid form, see: (a) Ichikawa, M.; Takahashi, M.; Aoyagi, S.; Kibayashi, C. *J. Am. Chem. Soc.* **2004**, *126*, 16553–16558. (b) Liu, J.; Wendt, N. L. K. *J. Org. Lett.* **2005**, *7*, 1007–1010. (c) Liu, D.; Ren, Z. G.; Li, H. X.; Lang, J. P.; Li, N. Y.; Abrahams, B. F. *Angew. Chem., Int. Ed.* **2010**, *49*, 4767–4770. (d) Shang, H.; Liu, J. H.; Bao, R. Y.; Cao, U.; Zhao, K.; Xiao, C. Q.; Zhou, B.; Hu, L. H.; Tang, Y. F. *Angew. Chem., Int. Ed.* **2014**, *53*, 14494–14498.
- (12) For reviews, see: (a) Singh, J. *Photochemistry and Pericyclic Reactions*, 3rd ed.; New Age Science: Tunbridge Wells, U.K., 2012; pp 229–261. (b) Zimmerman, H. E. *Pure Appl. Chem.* **2006**, *78*, 2193–2203. For examples of photoinduced skeletal rearrangements, see: (c) Zimmerman, H. E.; Schuster, D. I. *J. Am. Chem. Soc.* **1962**, *84*, 4527–4540. (d) Zimmerman, H. E.; Rieke, R. D.; Scheffer, J. R. *J. Am. Chem. Soc.* **1967**, *89*, 2033–2047. (e) Jones, G., II; Qian, X. H. *J. Phys. Chem. A* **1998**, *102*, 2555–2560.
- (13) In the attempt to effect the skeletal rearrangement of **6** with excess amounts of MgBr₂, we observed the formation of a small amount of **2** with a long reaction time. This result hinted at the possibility of the mechanism via zwitterion intermediates.
- (14) Based on the calculation study, the predicted distribution of **2** and **5** should fall into the range of 80:1 to 100:1, which is in agreement with the experimental results as well as their natural abundance.